Received: 31 July 2022 | Revised: 18 January 2023 | Accepted: 19 January 2023

DOI: 10.1111/mpp.13306

Molecular Plant Pathology WILEY

ORIGINAL ARTICLE

The potato StMKK5-StSIPK module enhances resistance to *Phytophthora* pathogens through activating the salicylic acid and ethylene signalling pathways

Hui Yang[1] | Xiaokang Chen[1] | Ruixin Yang[1] | Jing Cheng[1] | Yong Chen[1] | Matthieu H. A. J. Joosten[2] | Yu Du[1,3]

[1]College of Horticulture, Northwest A&F University, Yangling, China

[2]Laboratory of Phytopathology, Wageningen University, Wageningen, Netherlands

[3]Shaanxi Engineering Research Center for Vegetables, Yangling, China

Correspondence
Yu Du, College of Horticulture, Northwest A&F University, Yangling, Shaanxi 712100, China.
Email: yu.du@nwafu.edu.cn

Funding information
Chinese Universities Scientific Fund, Grant/Award Number: 2452018028 and 2452017069; National Natural Science Foundation of China, Grant/Award Number: 32072401 and 31701770

Abstract

Mitogen-activated protein kinase (MAPK) cascades play pivotal roles in plant responses to both biotic and abiotic stress. A screen of a *Nicotiana benthamiana* cDNA virus-induced gene silencing (VIGS) library for altered plant responses to inoculation with *Phytophthora infestans* previously identified an NbMKK gene, encoding a clade D MAPKK that we renamed as *NbMKK5*, which is involved in immunity to *P. infestans*. To study the role of the potato orthologous gene, referred to as *StMKK5*, in the response to *P. infestans*, we transiently overexpressed *StMKK5* in *N. benthamiana* and observed that cell death occurred at 2 days postinfiltration. Silencing of the highly conserved eukaryotic protein *SGT1* delayed the StMKK5-induced cell death, whereas silencing of the MAPK-encoding gene *NbSIPK* completely abolished the cell death response. Further investigations showed that StMKK5 interacts with, and directly phosphorylates, StSIPK. Furthermore, both StMKK5 and StSIPK trigger salicylic acid (SA)- and ethylene (Eth)-related gene expression, and co-expression of the salicylate hydroxylase NahG with the negative regulator of Eth signalling CTR1 hampers StSIPK-triggered cell death. This observation indicates that the cell death triggered by StMKK5-StSIPK is dependent on the combination of SA- and Eth-signalling. By introducing point mutations, we showed that the kinase activity of both StMKK5 and StSIPK is required for triggering cell death. Genetic analysis showed that StMKK5 depends on StSIPK to trigger plant resistance. Thus, our results define a potato StMKK5-SIPK module that positively regulates immunity to *P. infestans* via activation of both the SA and Eth signalling pathways.

KEYWORDS
ethylene, MAPK, *Phytophthora infestans*, plant resistance, salicylic acid

Hui Yang and Xiaokang Chen contributed equally to this work.

1 | INTRODUCTION

Potato (*Solanum tuberosum*) originates from South America and is one of the most important vegetable and staple food crops worldwide. Potato production is seriously threatened by various plant pathogens, among which the most notorious is *Phytophthora infestans*, the causal agent of potato late blight disease. This disease causes billions of dollars of losses yearly in potato production all over the world (Fry, 2008), and late blight disease management is dependent on spraying of chemicals, which causes environmental problems. Potato resistance breeding will help to control late blight disease in a cost-effective and ecofriendly way. Potato resistance breeding heavily relies on the presence of particular *NLR* genes (*nucleotide-binding leucine rich repeat* genes), also commonly known as *R* (*resistance*) genes. *NLR*s confer full resistance to strains of *P. infestans* that contain the corresponding *Avr* (*avirulence*) gene, making their avirulence race-specific. Attempts to grow disease-resistant potato cultivars carrying the appropriate *NLRs* to control *P. infestans* failed, as the pathogen can quickly adapt and overcome resistance (Ivanov et al., 2021). This feature is due to the plasticity of the genome of *P. infestans*, of which the core orthologous genes are located mainly in the less dynamic, gene-dense regions, while the *Avr*, or so-called effector-encoding, genes are located in the more dynamic, gene-sparse, repeat-rich regions (Haas et al., 2009). This provides *P. infestans* with the ability to evolve its effector genes rapidly when there is selection pressure as a result of plant resistance, thereby overcoming the resistance of novel introduced potato cultivars. Thus, the identification and characterization of novel race-specific disease resistance genes will be essential for improving potato resistance breeding.

Plant basal resistance conferred by plasma membrane-localized receptor-like kinases (RLKs) and receptor-like proteins (RLPs), also referred to as pattern recognition receptors (PRRs), plays an important part in nonrace-specific resistance (Jones & Dangl, 2006). Mitogen-activated protein kinase (MAPK) cascades function as important signalling modules downstream of RLPs and RLKs (Pitzschke et al., 2009), and this cascade is composed of an upstream MAPK kinase kinase (MAPKKK, MAP3K, or MEKK), a MAPK kinase (MAPKK, MAPK2K, MKK or MEK), and a downstream MAPK (MPK). On their activation by a matching ligand, plasma membrane-associated receptors activate a particular cytoplasmic MAPKKK by phosphorylation, which in its turn activates a MAPKK by phosphorylation of its conserved S/T-XXXXX-S/T (S, serine; T, threonine; X, any amino acid) motif, after which the activated MAPKK phosphorylates the TXY (T, threonine; X, any amino acid; Y, tyrosine) motif of a downstream MAPK, which then activates downstream transcription factors, enzymes or kinases by phosphorylating them (He et al., 2020; Zhang et al., 2018). MAPK cascades transmit and amplify external signals to downstream cytoplasmic and nuclear proteins to activate signalling in plant development, hormonal responses, and responses to biotic and abiotic stress (Komis et al., 2018). There are numerous reports showing interactions between MAPK cascades and proteins involved in plant hormone biosynthesis or signalling. For example, MAPK3 and MAPK6 were reported to regulate ethylene (Eth) biosynthesis, at the level of both gene transcription and protein stability. For this, these MAPKs phosphorylate the transcription factor WRKY33 to stimulate transcription of the 1-aminocyclopropane-1-carboxylate synthase (ACS)-encoding genes *ACS2* and *ACS6* in response to pathogen colonization (Li et al., 2012). Moreover, in *Arabidopsis thaliana* (Arabidopsis), MAPK3 and -6 also stabilize the ACS proteins to enhance Eth production (Liu & Zhang, 2004). The MAPKK9-MAPK3 and -6 combination was reported to regulate Eth and camalexin biosynthesis (Xu et al., 2008), whereas Arabidopsis MAPK12 negatively regulates auxin signalling (Smekalova et al., 2014). The MAPK SALICYLIC ACID-INDUCED PROTEIN KINASE (SIPK) was first identified as salicylic acid (SA)-induced protein kinase and was later shown to be involved in plant defence and hypersensitive response (HR) cell death by phosphorylating SGT1 (Hoser et al., 2013; Liu et al., 2016; Zhang & Liu, 2001). The potato StMAPK7 and StMAPKK1 combination positively or negatively regulates immunity to *P. infestans* by either up- or down-regulating SA-related signalling, respectively (Chen et al., 2021; Zhang et al., 2021).

Large-scale forward genetic studies, for example by chemical- or T-DNA-mediated mutagenesis, have greatly facilitated functional studies of Arabidopsis genes. However, functional genomics studies are difficult to perform in potato because of its tetraploid genome and extended generation cycle. Virus-induced gene silencing (VIGS) provides a powerful tool for performing large-scale functional analysis in crop plants that have a polyploid genome, a long generation cycle, and are difficult to transform (Gao & Shan, 2013). The VIGS technique is based on RNA-mediated posttranscriptional gene silencing, and avoids stable plant transformation and allows the knockdown of paralogous gene expression, thereby overcoming functional gene redundancy in polyploid plants (Burch-Smith et al., 2004). This method has, for example, been successfully applied in cotton for screening for resistance to Verticillium wilt (Gao et al., 2011). *P. infestans* has a narrow host range as it infects potato, tomato, and *Nicotiana benthamiana*, but not the model plant Arabidopsis. Therefore, screening of a *N. benthamiana* cDNA-VIGS library by *P. infestans* inoculation assays on randomly silenced *N. benthamiana* plants provides an alternative tool for the identification of genes involved in basal disease resistance or susceptibility, which can be exploited in resistance breeding.

According to the method described by Helderman et al. (2022) and Gao and Shan (2013), we previously used a *N. benthamiana* cDNA-VIGS library for screening for compromised basal disease resistance or for the identification of susceptibility genes to *P. infestans* (unpublished data). We observed that silencing of the *N. benthamiana MAPKK* gene *Niben101Scf01249g04006* results in an enhanced susceptibility to *P. infestans*. According to the phylogenetic tree of solanaceous MAPKK proteins, we renamed this gene as *NbMKK5*. To investigate the role of this MAPKK in potato resistance to *P. infestans* we cloned the potato ortholog *Sotub03g022560*. We observed that overexpression of StMKK5 induced cell death in *N. benthamiana* and found that this feature was dependent on both SA- and Eth-related signalling. Silencing of the gene encoding SIPK completely

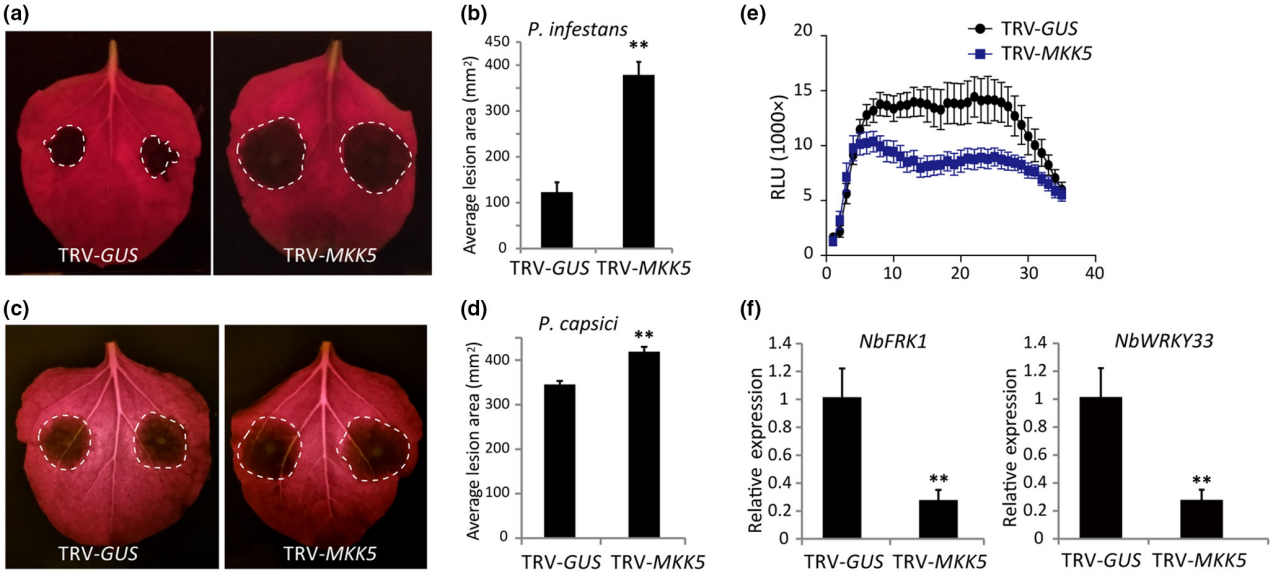

FIGURE 1 Silencing of *NbMKK5* in *Nicotiana benthamiana* promotes colonization by *Phytophthora* pathogens. (a, c) Representative images showing *Phytophthora infestans* (a) and *Phytophthora capsici* (c) lesion development on TRV-*GUS*- and TRV-*NbMKK5*-inoculated plants. (b, d) Average lesion areas on leaves of TRV-*GUS*- and TRV-*NbMKK5*-inoculated plants were determined at 6 days after inoculation (dai) for *P. infestans* and at 2 dai for *P. capsici*. Error bars show the standard errors from more than eight replicates. Asterisks indicate significant differences ($n \geq 8$; one-sided Student's *t* test, $^{**}p \leq 0.01$). (e) *NbMKK5*-silenced plants show a significant repression of the flg22-induced reactive oxygen species (ROS) production when compared to the control TRV-*GUS* plants. Middle leaves from 5-week-old TRV-*GUS*- and TRV-*NbMKK5*-inoculated plants were infiltrated with a solution of 10 μM flg22, after which ROS production was measured. RLU, relative luminescence units. (f) Relative expression of the *NbFRK1* and *NbWRKY33* genes in leaves of the TRV-*GUS*- and TRV-*NbMKK5*-inoculated plants were analysed by reverse transcription-quantitative PCR after infiltration of the flg22 solution. *Nbactin* gene expression was used for normalization. The expression levels of *NbFRK1* and *NbWRKY33* genes in GUS-GFP was set to 1. Asterisks indicate significant differences ($n = 3$; one-sided Student's *t* test, $^{**}p \leq 0.01$). Error bars represent the standard deviation from three technical replicates. The experiments were repeated three times, with similar results.

abolished StMKK5-triggered cell death, while silencing of the gene encoding the HSP90 chaperone-interacting protein SGT1 only delayed the onset of the cell death response, indicating that SIPK is the downstream signalling target of StMKK5. We further showed that StMKK5 phosphorylates, and interacts with, StSIPK and that StMKK5 depends on StSIPK to trigger potato immunity to *P. infestans*. Thus, our results have identified a MKK5-SIPK module from solanaceous plants that is part of a MAPK cascade that positively regulates immunity to *P. infestans*.

2 | RESULTS

2.1 | A random VIGS screen identifies NbMKK5 as a positive regulator of immunity of *N. benthamiana* to *P. infestans*

N. benthamiana is an ideal model host plant to study the molecular mechanisms of immunity of solanaceous plants against oomycetes belonging to the *Phytophthora* genus (Du et al., 2021; Li et al., 2022; Matsukawa et al., 2013; Shibata et al., 2016; Zhang et al., 2021). In our cDNA-VIGS screen in *N. benthamiana*, we tested in total 384 *Agrobacterium* colonies containing random TRV2 plasmids (unpublished data), and we found that VIGS driven by one *Agrobacterium* colony containing a TRV2 plasmid with an insert of which the nucleotide sequence matches with a *N. benthamiana MAPKK* gene (*Niben101Scf01249g04006*) resulted in an enhanced susceptibility to *P. infestans*. In our previous work, we performed a phylogenetic analysis of the Solanaceae MAPKK proteins and grouped them into four clades, clade A to clade D (Chen et al., 2021). We named all MAPKK proteins from potato, tomato, and *N. benthamiana* according to their phylogenetic relationship (Table S1), and *Niben101Scf01249g04006* was found to belong to the clade D of MAPKKs and we named it *NbMKK5*. To confirm the role of NbMKK5 in immunity to *Phytophthora* pathogens, we constructed a TRV-*NbMKK5* vector to silence *NbMKK5* in *N. benthamiana* and then tested these plants for altered susceptibility to the pathogens. Three weeks after VIGS inoculation, middle leaves were harvested for RNA isolation and reverse transcription-quantitative PCR (RT-qPCR) results showed that *NbMKK5* was efficiently silenced and furthermore the silenced plants showed a similar morphology as the control plants that were inoculated with TRV-*GUS* (*β-glucuronidase*) (Figure S1). Subsequently, zoospore suspensions from *P. infestans* and *Phytophthora capsici* were inoculated onto fully expanded leaves of the TRV-*NbMKK5*- or TRV-*GUS*-inoculated plants, and we observed that silencing of *NbMKK5* results in enhanced susceptibility to both pathogens when compared to the inoculated TRV-*GUS* control plants (Figure 1a–d).

MAPK cascades are major components downstream of receptors or sensors that transduce extracellular stimuli into intracellular to activate the pattern-triggered immunity (PTI) response in plants (Zhang & Zhang, 2022). To determine whether NbMKK5 also plays a role in a typical plant PTI response, we infiltrated leaves of the TRV-*NbMKK5*- and TRV-*GUS*-inoculated plants with a solution of 10 μM flg22, after which the level of the reactive oxygen species (ROS) burst was determined. We found that silencing of *NbMKK5* significantly suppressed the flg22-induced ROS burst when compared to the GUS control (Figure 1e). To investigate whether silencing of *NbMKK5* also inhibits PTI-related gene expression, leaves of the TRV-*NbMKK5*- and TRV-*GUS*-inoculated plants were infiltrated with the 10 μM flg22 solution and harvested 3 h later for RNA isolation. The RT-qPCR results showed that the expression of the PTI-responsive genes *FLG22-INDUCED RECEPTOR-LIKE KINASE 1* (*FRK1*) and *WRKY33*, encoding a transcription factor involved in disease resistance, was significantly repressed in the *NbMKK5*-silenced plants when compared to the control plants (Figure 1f).

To investigate whether the potato orthologue of *NbMKK5*, *StMKK5* (*Sotub03g022560*), plays a similar role in plant immunity, we cloned the coding region of *StMKK5* and translationally fused *GFP* to its 3′-end. Agroinfiltration of StMKK5-GFP (green fluorescent protein) into *N. benthamiana* leaves, at an OD_{600} of 0.3, was found to trigger a clear cell death at 2 days post-agroinfiltration (dpi) (Figure 2a) and 3,3′-diaminobenzidine (DAB) staining showed that transient StMKK5-GFP overexpression induced high amounts of H_2O_2 compared to the GUS-GFP control (Figure 2b). To check whether the kinase activity of StMKK5 is required for its ability to trigger cell death, we substituted the key lysine (K) residue by an arginine (R) residue to generate the kinase-dead mutant StMKK5^{K93R}. The results show that StMKK5^{K93R} completely lost its ability to trigger cell death (Figure 2c). To investigate whether StMKK5^{K93R} also lost the ability to activate plant immunity, we transiently expressed GUS-GFP or StMKK5^{K93R}-GFP in the left and right panels of *N. benthamiana* leaves and performed pathogen inoculation assays at 1 dpi. Because transient expression of wild-type StMKK5 triggers a fast and severe cell death, we could not take this construct along in our assay. We observed that StMKK5^{K93R}-GFP-expressing leaves developed similar lesions as the control, indicating that the kinase activity of StMKK5 is indeed essential for activating immunity to *P. infestans* (Figure 2c–e). Protein stability of StMKK5-GFP, StMKK5^{K93R}-GFP was shown by western blotting (Figure S2), and subcellular localization assays showed that StMKK5^{K93R}-GFP localized in the nucleus and in the cytoplasm of the plant cells (Figure S3a). Western blotting showed that the StMKK5^{K93R}-GFP fusion protein was intact and no free GFP was observed on the blot (Figure S3b).

2.2 | StMKK5 interacts with, and phosphorylates, potato StSIPK

The activation of MAPKs is one of the earliest signalling events on perception of both PAMPs and effectors (Meng & Zhang, 2013). It was reported that the cell death elicited by transient overexpression of *A. thaliana* defence-related MAPK kinases in *N. benthamiana* depends on SGT1 (Popescu et al., 2009). Additionally, it is known that BAK1 and SOBIR1 are required for HR induction and ETI triggered by the recognition of effectors (avirulence proteins) by the R proteins (Liebrand et al., 2013; Ma & Borhan, 2015; Postma et al., 2016). Consequently, to investigate in which signalling pathway StMKK5 participates, we silenced the RLK-encoding genes *BAK1* and *SOBIR1*, the MAPK cascade genes *MEK1*, *MEK2*, *SIPK*, and *WIPK*, the gene encoding the transcription factor *WRKY33*, the SA signalling-related gene *TGA2.2* (Ouyang et al., 2015), and the NLR signalling-related genes *SGT1* and *RAR1* (Figure 2f) by VIGS. The silencing efficiency of the various genes was detected by RT-qPCR and the results showed that all the genes were efficiently silenced (Figure S4). Three weeks after agroinfiltration with the various VIGS constructs, we transiently expressed StMKK5 to determine whether the cell death response was affected. Agroinfiltration of INF1, which is an effector of *P. infestans* that triggers cell death in *N. benthamiana*, was used as a control and we observed that silencing of *BAK1*, *SOBIR1*, and *SGT1* suppressed the INF1-induced cell death, which is an observation that matches earlier reports (Domazakis et al., 2018; Liu et al., 2016; Wang et al., 2010). In the control TRV-*GUS* plants, StMKK5 expression induced a robust cell death at 4 dpi, whereas the TRV-*SGT1* only showed slight cell death at 4 dpi, which increased to full cell death at 7 dpi (Figure S5). Silencing of *SIPK* completely abolished the StMKK5-induced cell death (Figure 2f), indicating that SIPK plays an essential role downstream of StMKK5. VIGS of all other genes did not affect the StMKK5-triggered cell death. Combining these results with the report that *N. benthamiana* SGT1 undergoes specific phosphorylation by SIPK (Hoser et al., 2013), we thus supposed that SIPK may act as a direct downstream signalling target of StMKK5. To confirm this, we cloned the potato orthologue StSIPK and performed firefly luciferase complementation imaging (LCI) assays to check for an interaction between StMKK5 and StSIPK. Because transient expression of StMKK5 triggers cell death, we decided to express the StMKK5^{K93R} kinase-dead mutant instead of wild-type StMKK5. We observed that StMKK5^{K93R} interacted with StSIPK, as co-expression of CLuc-StMKK5^{K93R} with StSIPK-NLuc restored the catalytic activity of luciferase (Figure 3a,b). To analyse whether StMKK5 phosphorylates StSIPK in planta, we transiently expressed StMKK5-GFP, GFP, and the kinase-dead mutant StMKK5^{K93R}-GFP in leaves of *N. benthamiana*. Total proteins were extracted at 2 dpi, and possible phosphorylation of NbSIPK was detected using α-pErk antibodies. The results show that only StMKK5, but not the kinase-dead version of StMKK5^{K93R} or the GFP control, phosphorylated NbSIPK. Furthermore, only NbSIPK was phosphorylated and not the other NbMAPKs (Figure 3c).

Possible direct phosphorylation of StSIPK by StMKK5 was subsequently investigated by in vitro phosphorylation assays. For this, His-GFP and His-StMKK5 proteins were incubated with GST-StSIPK and western blotting revealed that only co-incubation of StSIPK with StMKK5 resulted in phosphorylation of StSIPK (Figure 3d). To investigate whether NbSIPK is phosphorylated on treatment with flg22

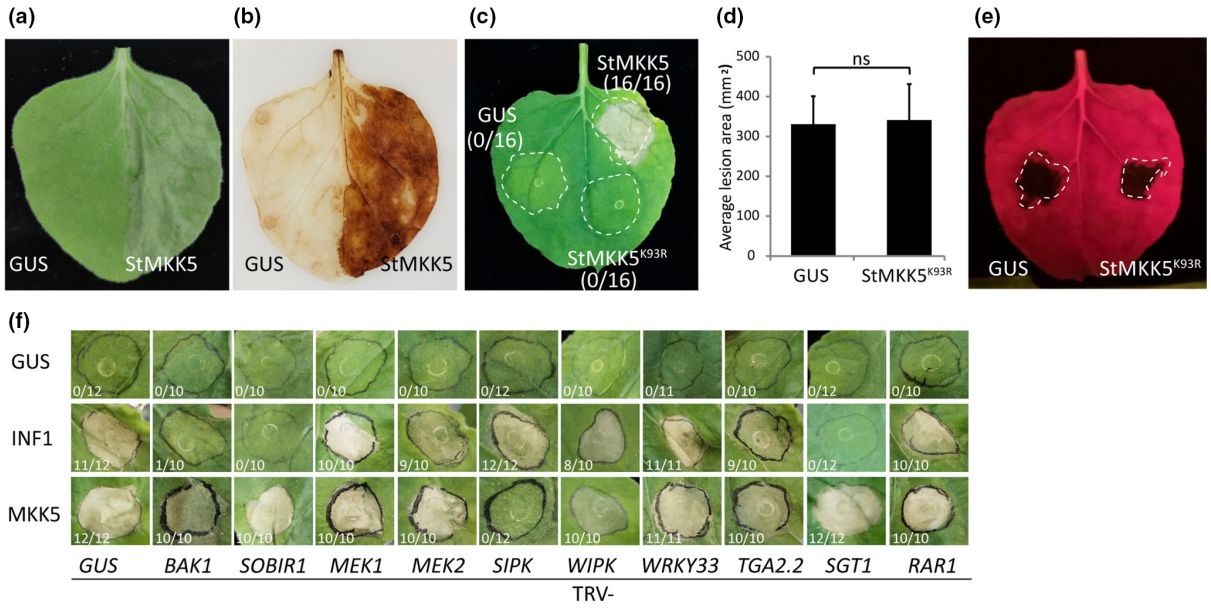

FIGURE 2 Overexpression of potato StMKK5 triggers a SIPK-dependent plant cell death in *Nicotiana benthamiana*. (a) GUS-GFP (left) and StMKK5-GFP (right) were agroinfiltrated into *N. benthamiana* leaves at an OD_{600} of 0.3, and pictures were taken at 2 days post-agroinfiltration (dpi). (b) H_2O_2 accumulation in the StMKK5-GFP-infiltrated leaf half, as shown by 3,3′-diaminobenzidine (DAB) staining. (c) StMKK5-GFP, but not the kinase-dead variant $StMKK5^{K93R}$-GFP, triggers cell death in *N. benthamiana* leaves. GUS-GFP, StMKK5-GFP, and $StMKK5^{K93R}$-GFP were infiltrated into *N. benthamiana* leaves and the picture was taken at 2 dpi. (d, e) Transient expression of kinase-dead $StMKK5^{K93R}$-GFP does not affect plant resistance to *Phytophthora infestans*. GUS-GFP and $StMKK5^{K93R}$-GFP were agroinfiltrated into *N. benthamiana* leaves, and at 1 dpi *P. infestans* zoospores were inoculated onto the leaves. Average lesion areas on GUS-GFP- and $StMKK5^{K93R}$-GFP-expressing leaves were determined (d) and a representative image showing *P. infestans* lesion development, taken at 6 dpi, is shown (e), and error bars represent the standard errors from more than 10 infection sites. Statistical analysis was performed using one-sided Student's *t* test. ns, nonsignificant differences. The experiments were repeated at least two times, with similar results. (f) StMKK5-GFP-triggered cell death is compromised in *SIPK*-silenced plants. StMKK5-GFP was transiently expressed in the different TRV-inoculated plants, at an OD_{600} of 0.1, and the development of cell death was monitored. Pictures were taken at 5 dpi. The ratios next to the infiltrated zones for (c) and (f) indicate the amount of agroinfiltrated sites showing cell death versus the total amount of agroinfiltrated sites.

and whether NbMKK5 is required for the flg22-triggered NbSIPK phosphorylation, we treated TRV-*GUS*-, TRV-*MKK5*- or TRV-*MEK2*-inoculated plants with flg22, and total proteins were extracted at 0 and 15 min after treatment. TRV-*MEK2* targets the clade C *MAPKK* genes *NbMKK4-2* and *NbMKK4-3* (*Niben101Scf14708g00019* and *Niben101Scf01283g02011*), which have been reported to be the upstream MAPKK proteins phosphorylating SIPK (Mase et al., 2012). We found that NbSIPK was phosphorylated on treatment with flg22, whereas silencing of *NbMKK5* and also of *NbMEK2* repressed the phosphorylation of NbSIPK (Figure 3e), suggesting that we have identified an additional MAPKK protein from clade D that phosphorylates SIPK, next to the MAPKK proteins from clade C.

2.3 | The StMKK5-StSIPK module positively regulates resistance to *Phytophthora* pathogens and triggers SA- and Eth-related cell death in *N. benthamiana*

To investigate the role of StSIPK in plant immunity, we transiently expressed StSIPK-GFP and the control GUS-GFP in *N. benthamiana* leaves and inoculated these with *P. capsici*. We observed that transient expression of StSIPK-GFP enhanced immunity to *P. capsici* (Figure 4a–c). To further confirm this observation, we silenced *NbSIPK* in *N. benthamiana* and found that basal resistance to *P. capsici* was compromised (Figure 4d–f). We also observed that transient expression of StSIPK-GFP triggered cell death in *N. benthamiana* when agroinfiltrated at an OD_{600} of 0.5, and this cell death was also associated with a massive accumulation of H_2O_2 in the infiltrated leaf tissue (Figure 4g,h). To test whether the kinase activity of StSIPK is required for its role in enhancement of plant immunity to *P. capsici* and triggering plant cell death, we created a kinase-dead StSIPK mutant ($StSIPK^{K92,93R}$) and observed that $StSIPK^{K92,93R}$ lost its ability to promote immunity to *P. capsici* and trigger plant cell death and H_2O_2 accumulation (Figure 4i–l). In addition, co-expressing StSIPK with the protein tyrosine phosphatase StPTP1 abolished the StSIPK-triggered cell death (Figure 4m,n), suggesting that the kinase activity of StSIPK is essential for triggering cell death.

To investigate in which signalling pathway the StMKK5-StSIPK module is involved, we transiently expressed GUS-GFP, StMKK5-GFP, and StSIPK-GFP, as well the kinase-dead version $StMKK5^{K93R}$-GFP, into leaves of *N. benthamiana* and determined whether SA-, jasmonic acid (JA)-, and/or Eth-responsive gene expression was induced. Overexpression of StMKK5 and StSIPK was found to

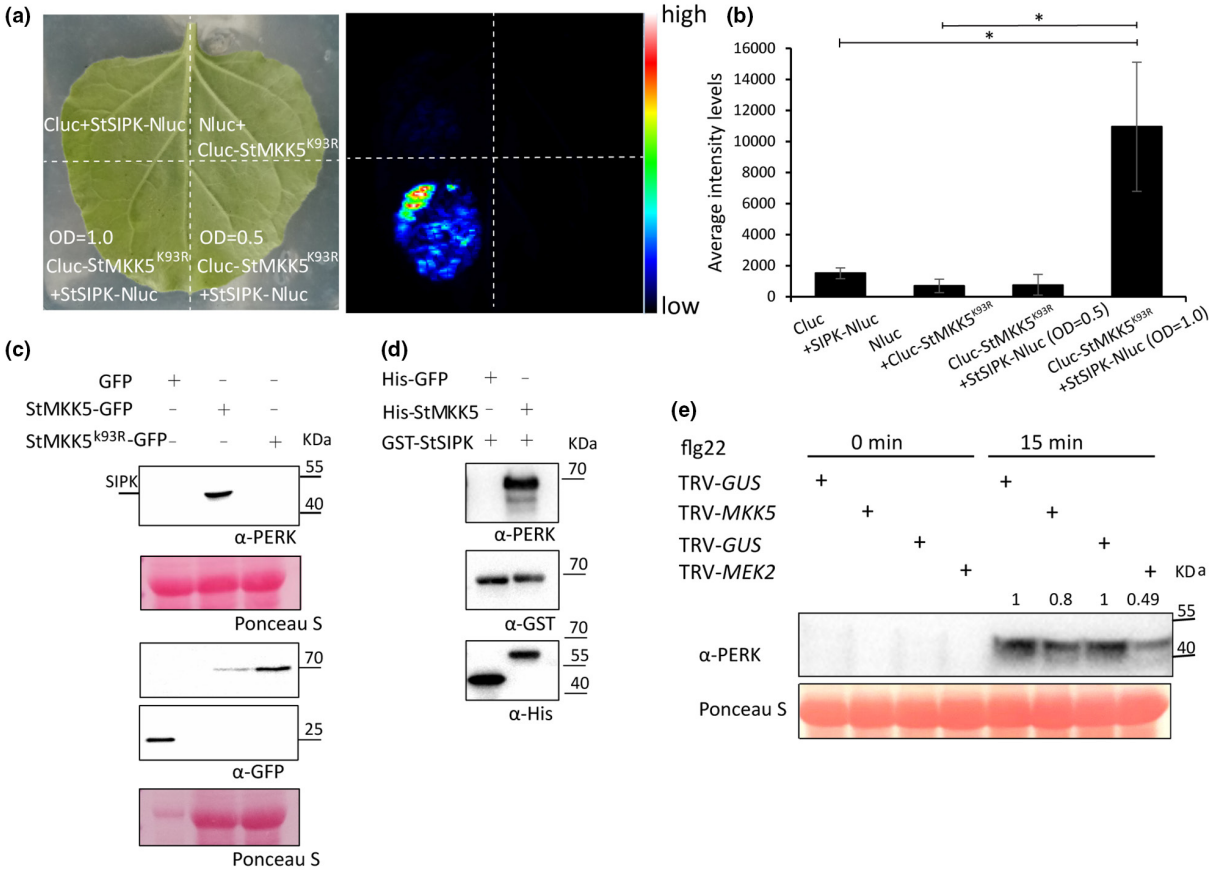

FIGURE 3 StMKK5 interacts with, and phosphorylates, StSIPK. (a) Firefly luciferase complementation imaging (LCI) assays employing co-expression of the indicated constructs show that StMKK5^{K93R} associates with StSIPK in planta. Pictures were taken using luminescence imaging at 2 days postinfiltration. Note that luminescence is only visible when StMKK5^{K93R} and StSIPK are co-expressed, in this case at an OD_{600} of 1.0. (b) Average intensity levels are calculated by using ImageJ software to quantify protein–protein interactions. Error bars show standard errors from three technical replicates. Asterisks indicate significant differences (one-sided Student's *t* test, $^*p \leq 0.05$). The experiments were repeated two times with each including three technical replicates. (c) StMKK5-GFP, but not StMKK5^{K93R}-GFP, phosphorylates NbSIPK in planta. GFP, StMKK5-GFP, and StMKK5^{K93R}-GFP were agroinfiltrated into *Nicotiana benthamiana* leaves, and at 2 dpi leaves were harvested for total protein isolation. GFP-fusion proteins were detected by western blots with α-GFP antibody. Phosphorylation of SIPK protein was detected using α-pErk antibody. Protein loading is indicated by Ponceau stain (Ponceau S). (d) StMKK5-GFP phosphorylates StSIPK in vitro. The recombinant proteins His-GFP or His-StMKK5 were incubated with GST-StSIPK, and phosphorylation of StSIPK was detected using α-pErk antibodies. (e) Flg22-triggered phosphorylation of NbSIPK is repressed in TRV-*NbMKK5*-inoculated plants. Leaves from TRV-*GUS*-, TRV-*NbMKK5*-, and TRV-*NbMEK2*-inoculated plants were treated with 10 μM flg22, after which total proteins were extracted at 0 and 15 min postinfiltration. Phosphorylation of MPK proteins was detected using α-pErk antibodies. Protein loading is indicated by Ponceau stain (Ponceau S). Note that there is also clear suppression of NbSIPK phosphorylation on inoculation with TRV-*NbMEK2*. Numbers indicate the ratio of the intensity of phosphorylated SIPK proteins normalized to RuBisCO. The experiments were repeated three times with similar results.

enhance both Eth- (*1-AMINOCYCLOPROPANE-1-CARBOXYLIC ACID SYNTHASE 6* [*ACS6*], *ACC OXIDASE 1* [*ACO1*], *ETHYLENE RESPONSE FACTOR 1*, and *5* [*ERF1 and ERF5*]) and SA-responsive gene expression (*PATHOGENESIS-RELATED PROTEIN 1*, *2* and *5* [*PR1*, *PR2*, and *PR5*]); however, this transient overexpression did not affect the expression of the JA-related gene *JASMONATE-RESISTANT 1* (*JAR1*) and inhibit the gene encoding the basic helix–loop–helix transcription factor (*MYC2*) (Figures 5 and S6).

To subsequently test whether StSIPK-induced cell death requires Eth-mediated signalling, we treated StSIPK-expressing leaves with the Eth biosynthesis inhibitor $CoCl_2$ (Hays et al., 2000) or co-expressed StSIPK or StMKK5 with the negative regulator of Eth signalling, AtCTR1 (At5g03730) (Gao et al., 2003). The results show that neither $CoCl_2$ nor AtCTR1 affected the StSIPK- or StMKK5-triggered cell death (Figure 6a,c,d). H_2O_2 accumulation at the StSIPK-agroinfiltrated sites was detected by DAB staining. We observed that a significant H_2O_2 generation was observed at all StSIPK-infiltrated sites (Figure 6b,e), suggesting that inhibition of Eth signalling is not sufficient to hamper StSIPK-induced cell death.

To investigate whether SA-related signalling is required for StSIPK-triggered cell death, we co-expressed StSIPK with the salicylate hydroxylase-encoding *NahG* gene. StSIPK-triggered cell death was not affected, while the H_2O_2 accumulation appeared to be slightly reduced by transient co-expression with NahG (Figure 6f,g),

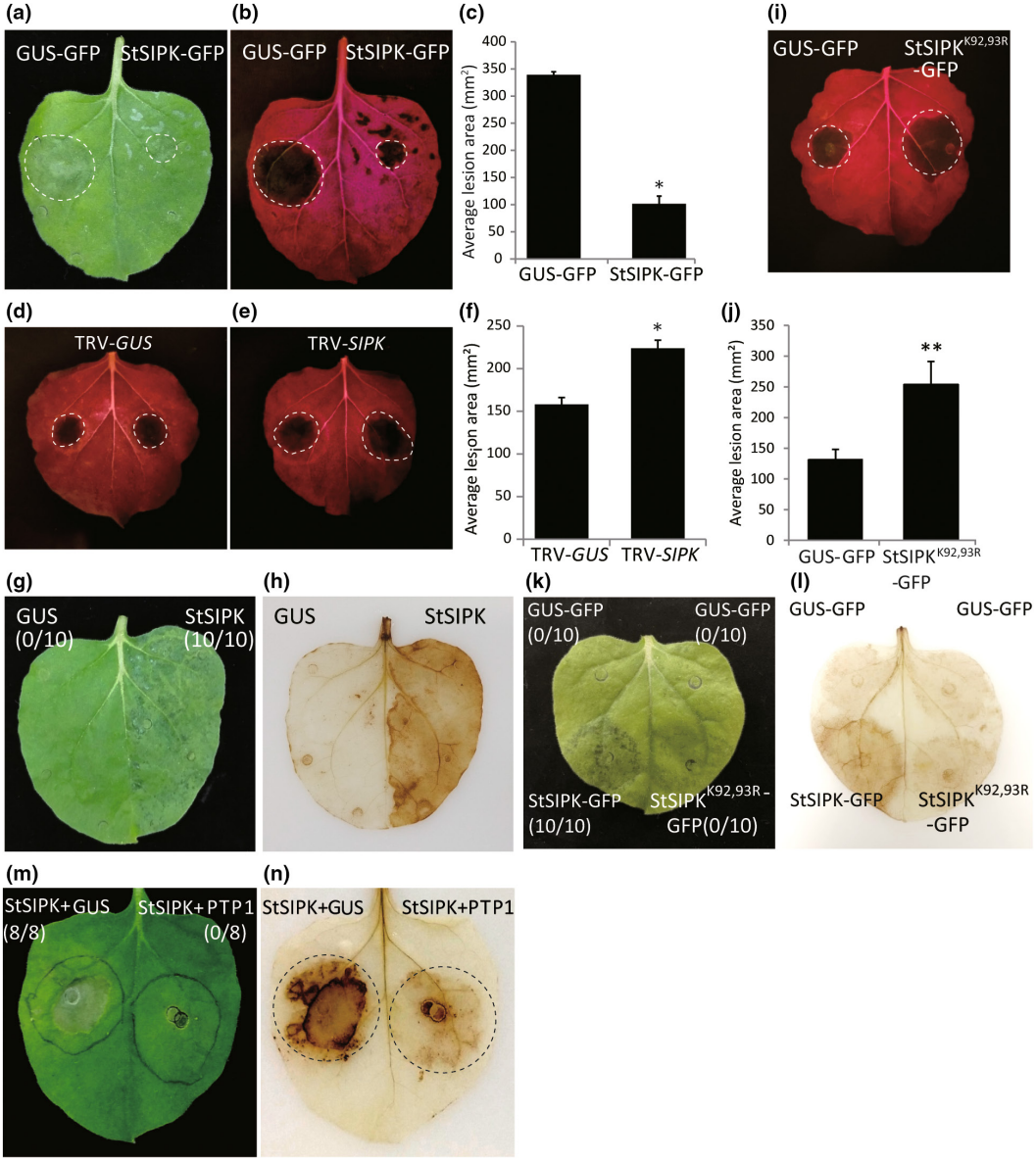

FIGURE 4 Overexpression of StSIPK promotes immunity to *Phytophthora capsici* and induces cell death. Representative images showing *P. capsici* lesion development on GUS-GFP- and SIPK-GFP-expressing leaves taken under normal light (a) or blue light (b) and on TRV-*GUS*- (d) and TRV-*SIPK*-inoculated (e) plants taken under blue light. (c, f) Average lesion areas on GUS-GFP- and SIPK-GFP-expressing leaves, and on leaves from TRV-*GUS*- and TRV-*SIPK*-inoculated plants, were determined at 3 days postinoculation (dpi). Error bars show standard errors from more than 10 replicates. Asterisks indicate significant differences ($n \geq 10$; one-sided Student's *t* test, $^{*}p \leq 0.05$). (g), Transient expression of StSIPK at an OD_{600} of 0.5 induces a weak cell death in *Nicotiana benthamiana* leaves. The picture was taken at 5 dpi. (h) 3,3′-diaminobenzidine (DAB) staining showing the accumulation of H_2O_2 in the StSIPK-GFP infiltrated leaf half. (i, j) Overexpression of the kinase dead mutation $StSIPK^{K92,93R}$ does not trigger increased immunity to *P. capsici*. Representative images, taken under blue light (i), show lesion development on the GUS-GFP- and $StSIPK^{K92,93R}$-GFP-expressing leaves. Lesion diameters were determined at 3 dpi, and the average lesion areas (mm^2) are shown in the graphs (j). Error bars show standard errors from more than 10 infection sites. Asterisks indicate significant differences ($n \geq 10$; one-sided Student's *t* test, $^{**}p \leq 0.01$). (k, l) $StSIPK^{K92,93R}$-GFP has lost its ability to trigger cell death. (k) The GUS-GFP, StSIPK-GFP, and $StSIPK^{K92,93R}$-GFP expressing leaves were photographed at 5 dpi. (l) H_2O_2 accumulation at the infiltrated sites with DAB staining. (m, n) StSIPK-triggered cell death (m) and reactive oxygen species accumulation (n) are suppressed on co-expression with the phosphatase StPTP1. The ratios next to the infiltrated zones show the number of infiltrated sites that developing cell death versus the total number of infiltrated sites (g, k, m) at 5 dpi. The experiments were repeated three times with similar results.

which indicates that repression of SA-signalling is also not sufficient for suppression of the StSIPK-induced cell death. To analyse whether StSIPK-triggered cell death is dependent on both SA- and Eth- signalling, we co-expressed StSIPK with both CTR1 and NahG, or treated the StSIPK and NahG co-expressing leaves with $CoCl_2$, and the results show that the StSIPK-induced cell death was significantly abolished in CTR1 and NahG or $CoCl_2$ and NahG-treated leaves (Figure 6h,i). StSIPK- and StMKK5-triggered cell death was

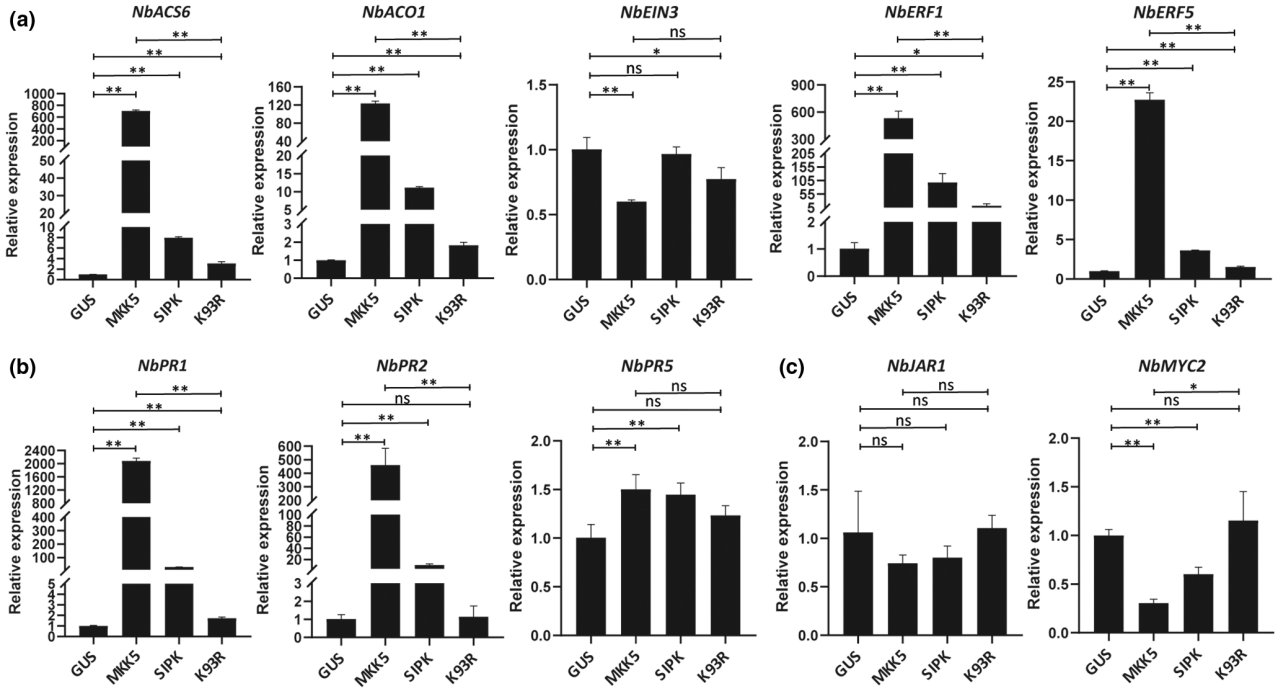

FIGURE 5 Transient expression of both StMKK5 and of StSIPK activates plant ethylene (Eth)- and salicylic acid (SA)-related signalling. GUS-GFP (GUS), StMKK5-GFP (MKK5), StSIPK-GFP, and StMKK5^{K93R}-GFP (K93R) were agroinfiltrated into leaves of *Nicotiana benthamiana* plants and harvested for RNA extraction at 2 days post-agroinfiltration (dpi). The relative expression levels of Eth-signalling marker genes *ACS6*, *ACO1*, *EIN3*, *ERF1*, and *ERF5* (a), the SA-signalling marker genes *PR1*, *PR2*, and *PR5* (b), and the jasmonic acid (JA)-signalling-related genes *JAR1* and *MYC2* (c) were determined by reverse transcription-quantitative PCR. *Nbactin* gene expression was used for normalization. The expression levels of Eth signalling-related genes, SA marker genes, and JA signalling-related genes in GUS-GFP were set to 1. Asterisks indicate significant differences ($n = 3$; one-sided Student's *t* test, $^{*}p \le 0.05$, $^{**}p \le 0.01$; ns, nonsignificant differences). Error bars represent the standard deviation from three technical replicates. The experiments were repeated three times with similar trends observed. Note that *EIN3* expression was not up-regulated on transient expression of StMKK5 and StSIPK. In some cases the kinase dead StMKK5^{K93R} shows significant difference compared to the GUS control, but the differences between StMKK5 and StMKK5^{K93R} are obvious.

quantified by relative ion leakage assays, and only CTR1 and NahG or $CoCl_2$ and NahG co-expression significantly reduced the ion leakage triggered by StSIPK expression (Figure 6j–l). These results suggest that StSIPK-triggered cell death is dependent on both SA and Eth signalling.

To further confirm this observation, we constructed constitutively activate (CA) StSIPK-CA (StSIPK$^{D218G,\ E222A}$) and performed similar cell death assays. The results show that none of CTR1, $CoCl_2$, and NahG was sufficient to repress StSIPK-CA-triggered cell death; however, co-expression of CTR1 and NahG with StSIPK-CA, or treatment of the NahG and StSIPK-CA-expressing leaves with $CoCl_2$, repressed the StSIPK-CA-triggered cell death (Figure S7a–f).

As shown in Figure S5, the StMKK5-triggered cell death was delayed in *SGT1*-silenced plants, and we therefore examined whether the cell death induced by SIPK is dependent on SGT1. By transient expression of GUS-myc and SIPK-CA-myc in TRV-*NbSGT1*- and TRV-*GUS*-inoculated plants, we observed that the SIPK-CA-induced cell death was abolished in *NbSGT1*-silenced plants (Figure S8), indicating a common signalling component is dependent on StMKK5 and StSIPK.

2.4 | MKK5 functions upstream of SIPK

We then further investigated whether StMKK5 requires SIPK to activate Eth- and SA-related immunity by checking Eth- and SA-related gene expression and lesion development on TRV-*NbSIPK*- or TRV-*GUS*-inoculated plants, on transient expression of GUS or StMKK5. One day after agroinfiltration, leaves were harvested for total RNA isolation or inoculation assays. Eth- and SA-related gene expression was measured by RT-qPCR analysis, and we observed that expression of StMKK5 induced Eth- and SA-related gene expression in the control TRV-*GUS* plants, whereas in the TRV-*NbSIPK* plants expression of StMKK5 promoted neither Eth- nor SA-related gene expression (Figure 7a). Lesion development was quantified at 2 days after *P. capsici* inoculation and in the TRV-*GUS* plants lesions were observed at GUS-expressing sites, whereas StMKK5 triggered cell death in these plants. In the TRV-*NbSIPK* plants, StMKK5 did not trigger cell death and the lesion areas were similar on the GUS- and StMKK5-expressing leaf halves, indicating that StMKK5-triggered plant immunity requires StSIPK and that StMKK5 functions upstream of StSIPK (Figure 7b,c).

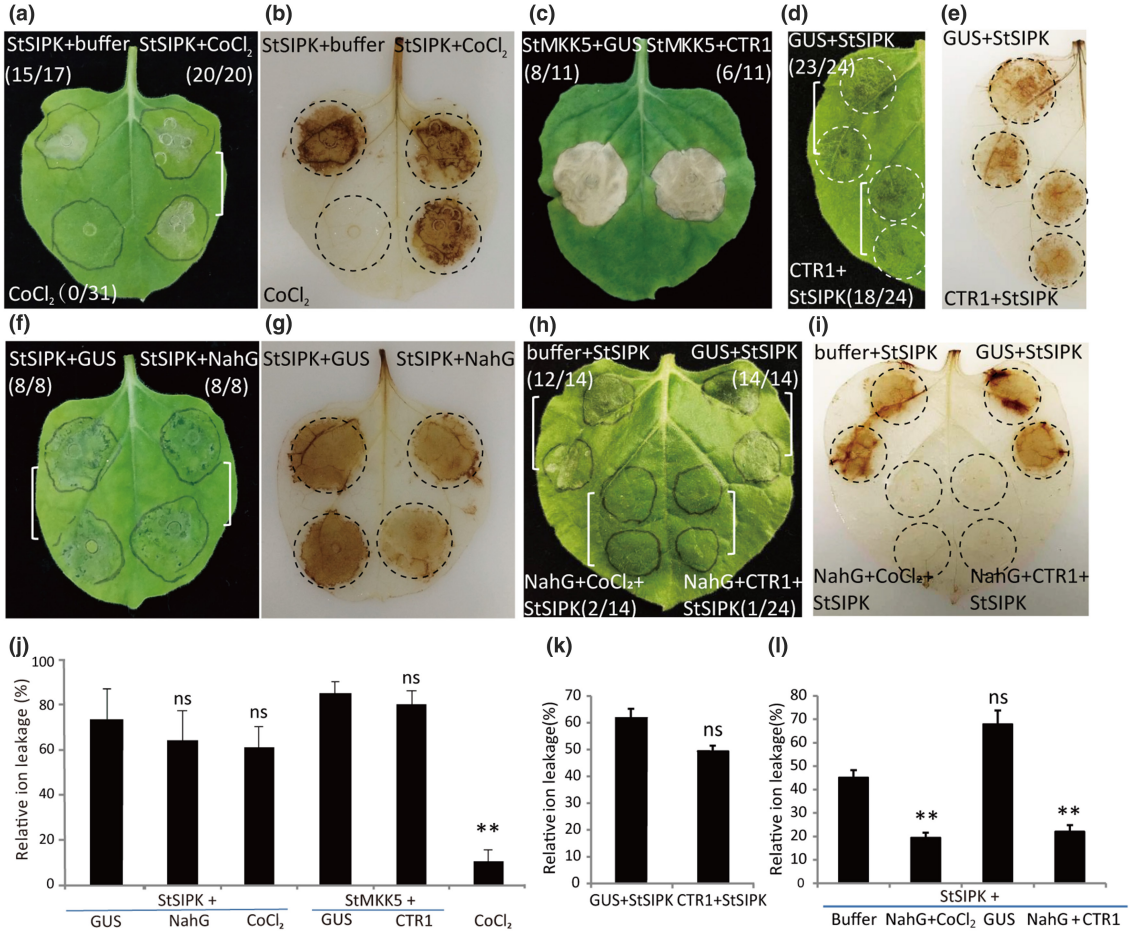

FIGURE 6 Repression of both ethylene (Eth) and salicylic acid (SA) signalling abolish the StSIPK-triggered plant cell death. (a, b) Treatment with the Eth biosynthesis inhibitor $CoCl_2$ does not affect StSIPK-induced cell death. StSIPK was agroinfiltrated into the leaves of *Nicotiana benthamiana* at an OD_{600} of 0.5. $CoCl_2$ was dissolved in liquid Murashige and Skoog (MS) medium and a solution of 100 μM $CoCl_2$ or liquid MS was infiltrated into the leaves of *N. benthamiana* at 1 day post-agroinfiltration (dpi). Cell death was photographed at 5 dpi. (c–e), The negative regulator of Eth signalling CTR1 does not hamper StMKK5- or StSIPK-induced cell death or reactive oxygen species (ROS) production. StMKK5 or StSIPK was co-expressed with GUS or the CTR1, with a final OD_{600} of 0.5 (StSIPK) or 0.1 (StMKK5) and cell death was photographed at 5 dpi. (f, g) The salicylate hydroxylase NahG does not hamper StSIPK-induced cell death. StSIPK was co-expressed with GUS or NahG in *N. benthamiana* leaves, with a final OD_{600} of 0.5, and cell death was photographed at 5 dpi. (h, i) Repression of both Eth- and SA-signalling abolish the StSIPK-triggered plant cell death. StSIPK was co-expressed in *N. benthamiana* leaves with $CoCl_2$ or CTR1 in the presence of NahG. (b, e, g, i), 3,3′-diaminobenzidine (DAB) staining showing the accumulation of ROS at StSIPK-GFP-agroinfiltrated sites. (j, k, l) Quantification of cell death triggered by StSIPK and StMKK5 by ion leakage assays. Relative ion leakage was measured and calculated at 5 dpi. One-sided Student's *t* test was used to assess significance: $^{*}p \leq 0.05$, $^{**}p \leq 0.01$; ns, nonsignificant differences. Error bars indicate the *SD* from three technical replicates. The experiments were repeated three times, with similar results. The ratios next to the infiltrated zones for (a), (c), (d), (f), and (h) indicate the amount of agroinfiltrated sites showing cell death versus the total amount of agroinfiltrated sites.

3 | DISCUSSION

There are plenty of reports describing the role of MAPK cascades in plant immunity. However, the number of reports on the role of solanaceous MAPKs in immunity to different pathogens is relatively limited. Our research identified a new MAPKK-MAPK module in potato that activates both Eth- and SA-related signalling to trigger immunity to *Phytophthora* pathogens. To identify resistance or susceptibility factors to the late blight pathogen *P. infestans*, an *N. benthamiana* cDNA-VIGS library was screened and we previously identified a MAPKK (unpublished data), referred to as NbMKK5, that plays a positive role in immunity, as VIGS of the encoding gene results in a significant enhancement of disease susceptibility.

We cloned the potato orthologous *StMKK5* gene and transiently expressed it in *N. benthamiana* leaves. We observed that overexpression of StMKK5 triggered a clear cell death response. By silencing some well-known signalling components in *N. benthamiana*, we found that the StMKK5-triggered cell death was delayed in *SGT1*-silenced plants and was completely abolished in *NbSIPK*-silenced plants, which indicates that StMKK5-triggered cell death is an HR-like programmed cell death, which partially depends on SGT1, whereas SIPK is an important downstream signalling component of StMKK5. To confirm whether the downstream SIPK depends

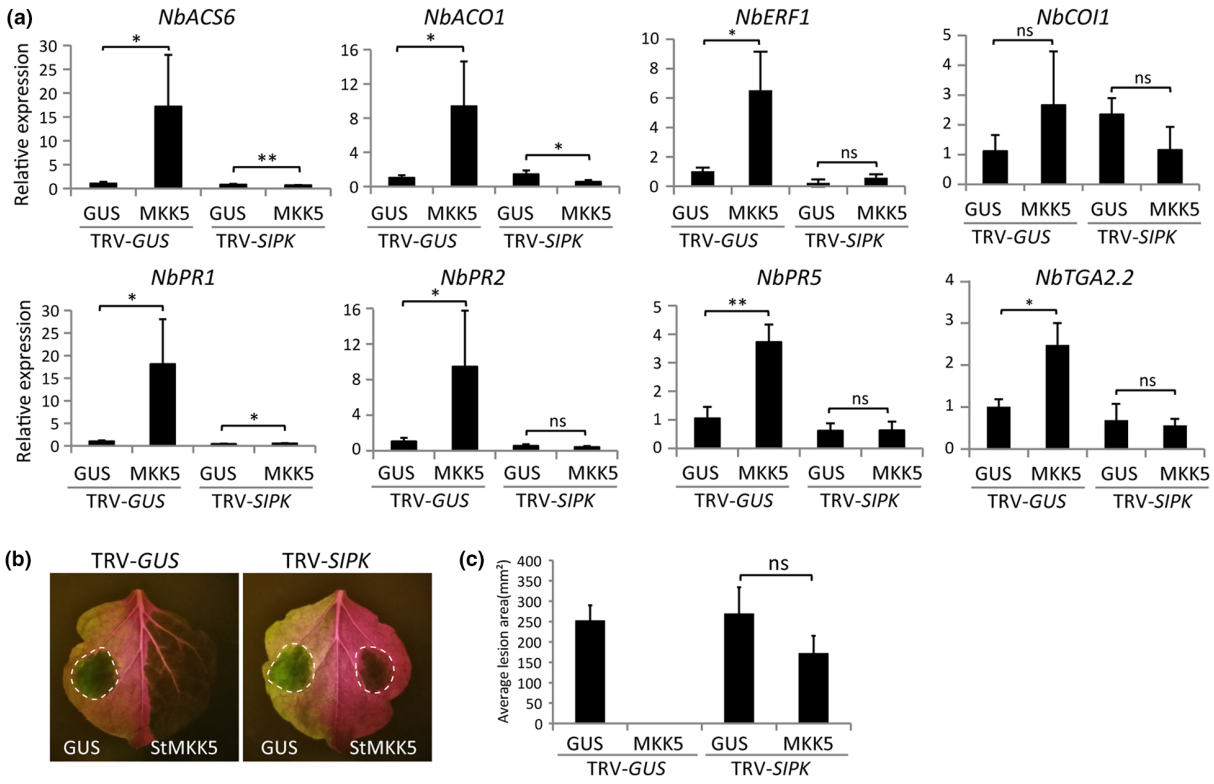

FIGURE 7 StSIPK is a downstream signalling component of StMKK5. (a) StMKK5 induced ethylene (Eth)- and salicylic acid (SA)-related gene expression is abolished in *SIPK*-silenced plants. GUS-GFP and StMKK5-GFP were transiently expressed in leaves of TRV-*GUS*- and TRV-*SIPK*-inoculated plants and at 2 days post-agroinfiltration leaves were harvested for RNA extraction. The relative expression level of Eth- and SA-related genes was analysed by reverse transcription-quantitative PCR, for which *Nbactin* expression was used for normalization. Error bars show the standard errors from three technical replicates (one-sided Student's *t* test, $^{*}p \le 0.05$, $^{**}p \le 0.01$; ns, nonsignificant differences). (b) StMKK5 requires StSIPK for activating plant resistance to *Phytophthora infestans*. GUS-GFP and StMKK5-GFP were agroinfiltrated into the left and right panels of leaves of TRV-*GUS*- and TRV-*SIPK*-inoculated leaves, respectively. At 1 day post-agroinfiltration, the infiltrated leaves were inoculated with a *Phytophthora capsici* zoospore suspension. Lesion development is shown by pictures taken under blue light, at 2 days after infection. Note that StMKK5-GFP triggers cell death in leaves of the TRV-*GUS*-inoculated plants. (c) Average lesion areas (mm^2) of the inoculated plants described in (b). Error bars show the standard errors (one-sided Student's *t* test in (c); ns, nonsignificant differences, $n \ge 10$). The above experiments were repeated three times with similar patterns shown in each time.

on the common signalling component SGT1 when inducing cell death, StSIPK-CA was expressed in TRV-*SGT1* and TRV-*GUS*. As expected, silencing of *SGT1* abolished StSIPK-CA-induced cell death (Figure S8), further showing that SIPK acts as the downstream component of StMKK5. This observation is further supported by in vivo and in vitro interaction and phosphorylation assays. We were able to show that StMKK5 interacted with StSIPK in LCI assays, whereas our in vitro and in vivo kinase assays confirmed a direct phosphorylation of StSIPK/NbSIPK by StMKK5 (Figure 3).

The potato genome encodes five *MAPKK* genes (*StMKK1* [*Sotub12g010200*], *StMKK2* [*Sotub03g033030*], *StMEK1* [*Sotub03g024510*, now renamed to *StMKK3* in this study], *StMEK2* [*Sotub03g034170*, renamed as *StMKK4* in this study], and *StMKK5* [*Sotub03g022560*]), but only two of them have been reported to play a role in regulating potato immunity. *StMKK1* was reported to negatively regulate potato immunity to biotrophic and hemibiotrophic pathogens (Chen et al., 2021; Du et al., 2021), whereas *NbMEK2* is involved in immunity to *P. infestans* triggered on overexpression of the leucine-rich repeat receptor-like kinase *StLRRK1* (Wang et al., 2018). The constitutively active StMEK1^{DD} protein, which is the potato orthologue of NtMEK2, triggers an HR-like cell death in *N. benthamiana* (Katou et al., 2003). Here, we found that StMKK5 positively regulates immunity to *Phytophthora* pathogens. Our results show that StMKK5, in combination with its downstream signalling target StSIPK, induces both SA- and Eth-related immune signalling in *N. benthamiana* (Figure 5). The role of SA in immunity of potato to *P. infestans* has been reported (Chen et al., 2021; Zhang et al., 2021), but the role of Eth in potato immunity to *P. infestans* is not well studied. It has been reported earlier that exogenous Eth treatment activates immune responses in the late blight disease resistant potato genotype SD20, indicating that Eth does participate in the resistance of potato to *P. infestans* (Yang et al., 2020). In most cases it is observed that SA antagonizes JA/Eth (Li, Han et al., 2019; Van der Does et al., 2013), but some exceptions have been observed. For example, tomato SlMKK2 and SlMKK4 activate both SA- and JA-related signalling to confer resistance to the necrotrophic pathogen *Botrytis cinerea*, which indicates that SA and JA/Eth might function synergistically to enhance plant immunity (Li, Zhang et al., 2014). Mase et al. (2012) reported that

the *Alternaria alternata* pathogenicity factor AAL-induced cell death was abolished in *MEK2*-silenced *Nicotiana umbratica* plants. MEK2-SIPK/WIPK modules play an essential role in Eth biosynthesis, and treatment with Eth recovers the AAL-induced cell death in *MEK2*-silenced *N. umbratica* plants. However, Eth cannot recover cell death in *SIPK*- or *WIPK*-silenced *N. umbratica*, which indicates that SIPK and WIPK play additional roles as well as those in Eth signalling. Indeed, a recent report on pathogen resistance of soybean showed that the GmMKK4-GmMPK6 module, of which the latter component is the orthologue of SIPK in soybean, interacts with, and phosphorylates, the ERF transcription factor GmERF113 to trigger PR1 and PR10 expression and immunity to *Phytophthora sojae* (Gao et al., 2022). Our research shows that StSIPK is phosphorylated and activated by the novel identified MAPKK StMKK5, and both StMKK5 and StSIPK play a role in SA- and Eth-related signalling (Figures 3–5). Inhibition of either Eth biosynthesis by treatment with $CoCl_2$ or SA signalling by transient expression of NahG did not inhibit the cell death induced by StSIPK or StMKK5 (Figure 6), while co-expressing StSIPK with both CTR1 and NahG, or treating the StSIPK and NahG co-expressing leaves with $CoCl_2$ inhibited the cell death (Figure 6h,i,l), indicating that SA and Eth signalling may function redundantly in mediating cell death, or additional signalling components next to SA and Eth are involved in the cell death phenotype. Our further studies show that silencing of *NbSIPK* completely inhibited the StMKK5-induced SA- and Eth-related gene expression, and abolished StMKK5-triggered cell death and immunity to *P. infestans*. Thus, our research and earlier reports indicate that SIPK is regulated by different MKK proteins to participate in different hormone signalling pathways. Further investigation of downstream signalling targets of potato StSIPK will help to reveal how the StMKK5-StSIPK module regulates both the SA- and Eth-dependent defence signalling pathways.

4 | EXPERIMENTAL PROCEDURES

4.1 | Vector construction

The coding regions from *StMKK5* (*Sotub03g022560*) and *StSIPK* were amplified from cDNA generated from potato cultivar Desiree. For transient expression assays, the coding regions of *StMKK5* and the kinase-dead mutant $StMKK5^{K93R}$ were translationally fused to GFP by cloning the inserts into the pART27-CGFP vector using the *Xho*I and *Hin*dIII sites to generate the *StMKK5-GFP*- and $StMKK5^{K93R}$-*GFP*-plasmids. *StSIPK* was cloned into the pART27-C4myc vector using *Xho*I and *Hin*dIII sites to generate the StSIPK-myc plasmid. The plasmids used for firefly luciferase complementation imaging (LCI) assays were generated by cloning of the $StMKK5^{K93R}$ and *StSIPK* coding regions into the CLuc-pCAMBIA and pCAMBIA-NLuc vectors (Chen et al., 2008), respectively, using the *Kpn*I and *Sal*I sites to generate the CLuc-$StMKK5^{K93R}$ and StSIPK-NLuc plasmids. For in vitro kinase activity assays, *GFP* and *StMKK5* were cloned into the pET32a vector using the *Bam*HI and *Sal*I sites to generate the His-GFP and His-StMKK5 plasmids, respectively. *StSIPK* was cloned into the pGEX-6P-1 vector using the *Bam*HI and *Sal*I sites to generate the GST-StSIPK plasmid.

4.2 | RNA isolation and RT-qPCR

The EZNA Plant RNA Kit (OMEGA Bio-tek), was used for total RNA extraction. One microgram of total RNA was used to synthesize the first-strand cDNA according to the manufacturer's instructions (PrimeScript RT reagent Kit; TaKaRa). The detailed descriptions of RT-qPCR assay are shown in Method S1. Primer pairs used for RT-qPCRs are shown in Table S2.

4.3 | Plant growth conditions and pathogen inoculation assays

Plants were grown under standard glasshouse conditions. Four- to five-week-old *N. benthamiana* were used for infection assays. For *Phytophthora* pathogens infection, the *P. infestans* isolate 14-3-GFP and *P. capsici* isolate BS11-1 were cultured, and infection assays were performed as described methods previously (Du et al., 2021; Li, Wang et al., 2019). Full descriptions are included in Method S2.

4.4 | VIGS and agroinfiltrations

The *N. benthamiana* cDNA-VIGS library was constructed as described by Helderman et al. (2022). For the VIGS screen, *Agrobacterium tumefaciens* C58C1 was used, and we mixed five agrobacterium strains, each containing a random cDNA insert in the TRV2 plasmid, and added this mix to an agrobacterium suspension with TRV1 at a 1:1 ratio before infiltrating into the leaves of 2-week-old *N. benthamiana* plantlets. The library was kept in 96-well plates and 96 different TRV2 plasmids were screened in the form of 20 mixes in one round. For each individual mix, five *N. benthamiana* plantlets were used. For those mixes resulting in an increased or decreased susceptibility to *P. infestans* on infiltration, we performed a second round of screening by combining each individual TRV2 strain from that mix with TRV1 and again performing *P. infestans* inoculation assays at 3 weeks after infiltration of the agrobacterium suspensions.

For confirming the role of MKK5 in the resistance response of *N. benthamiana*, VIGS inoculation and transient expression assays were used as described by Du et al. (2021). Full descriptions are included in Method S3. The silencing efficiency was determined by RT-qPCR using the primers shown in Table S2.

4.5 | Firefly luciferase complementation imaging assays

The firefly luciferase complementation imaging assays were performed according to the protocol described by Chen et al. (2008).

4.6 | ROS burst assays

Leaf discs taken from fully expanded middle leaves of 4- to 5-week-old *N. benthamiana* plants were treated with a 10 μM solution of bacterial flg22, and ROS burst analysis was performed as described previously by Li, Li et al. (2014).

4.7 | Western blot analysis

Extracted total proteins were separated on 10% SDS-PAGE gels before being transferred to PVDF membranes (Roche) for immune detection. Full descriptions are included in Method S4.

4.8 | Recombinant protein purification

His-GFP, His-StMKK5, and GST-StSIPK constructs were transformed to *Escherichia coli* BL21-CodonPlus (DE3). Proteins were purified according to the method described by Li, Li et al. (2014).

4.9 | In vivo and in vitro phosphorylation assays

In vitro phosphorylation assays were performed by incubation of purified His-GFP (control, 2 μg) or His-StMKK5 (2 μg) proteins with purified GST-StSIPK (2 μg) for 30 min at 30°C in reaction buffer (25 mM Tris–HCl pH 7.5, 10 mM $MgCl_2$, 1 mM dithiothreitol, and 100 μM dATP). For in vivo phosphorylation assays, the middle leaves of TRV-*GUS*-, TRV-*MKK5*-, and TRV-*MEK2*-inoculated plants were infiltrated with 10 μM flg22 and total proteins were extracted at 0 and 15 min after infiltration. GTEN buffer (10% [vol/vol] glycerol, 25 mM Tris–HCl [pH 7.5], 1 mM EDTA, and 150 mM NaCl), with 0.2% Nonidet P-40, protease inhibitor cocktail (1 tablet for 50 mL GTEN), and phosphatase inhibitor cocktails 2 and 3 (Sigma) was used for total protein extraction, and anti-pErk (#4370, Cell Signalling) antibodies were used to detect MAPK activation.

4.10 | DAB staining and ion leakage assays

N. benthamiana leaves were harvested at 5 dpi and incubated with DAB staining solution (1 mg/ml DAB, dissolved in Milli-Q water and using HCl to adjust the pH to 3.7) overnight. Subsequently, the leaves were washed with water and then incubated in 70% ethanol to remove the chlorophyll before pictures were taken. Relative ion leakage was measured as described by Bouwmeester et al. (2014).

AUTHOR CONTRIBUTIONS

Y.D. designed the research. H.Y., X.C., R.Y., J.C., and Y.C. performed the experiments and analysed the data. M.H.A.J.J. provided the VIGS library. Y.D. wrote the manuscript and M.H.A.J.J. revised the manuscript. All authors reviewed the manuscript.

ACKNOWLEDGEMENTS

The authors are very grateful to Min-Rong Luo of College of Horticulture, Northwest A&F University for assistance with Chemiluminescence Gel Imaging System. This work was supported by the National Natural Science Foundation of China (32072401, 31701770) and the Chinese Universities Scientific Fund (2452018028 and 2452017069).

CONFLICT OF INTEREST STATEMENT

Authors declare that they have no competing interests.

DATA AVAILABILITY STATEMENT

All data are available in the main text or in the supplementary materials.

ORCID

Matthieu H. A. J. Joosten https://orcid.org/0000-0002-6243-4547

Yu Du https://orcid.org/0000-0002-3512-0200

REFERENCES

Bouwmeester, K., Han, M., Blanco-Portales, R., Song, W., Weide, R., Guo, L. et al. (2014) The *Arabidopsis* lectin receptor kinase LecRK-I.9 enhances resistance to *Phytophthora infestans* in solanaceous plants. *Plant Biotechnology Journal*, 12, 10–16.

Burch-Smith, T.M., Anderson, J.C., Martin, G.B. & Dinesh-Kumar, S.P. (2004) Applications and advantages of virus-induced gene silencing for gene function studies in plants. *The Plant Journal*, 39, 734–746.

Chen, H., Zou, Y., Shang, Y., Lin, H., Wang, Y., Cai, R. et al. (2008) Firefly luciferase complementation imaging assay for protein–protein interactions in plants. *Plant Physiology*, 146, 368–376.

Chen, X., Wang, W., Cai, P., Wang, Z., Li, T. & Du, Y. (2021) The role of the MAP kinase-kinase protein StMKK1 in potato immunity to different pathogens. *Horticulture Research*, 8, 117.

Domazakis, E., Wouters, D., Visser, R.G.F., Kamoun, S., Joosten, M.H.A.J. & Vleeshouwers, V.G.A.A. (2018) The ELR-SOBIR1 complex functions as a two-component receptor-like kinase to mount defense against *Phytophthora infestans*. *Molecular Plant-Microbe Interactions*, 31, 795–802.

Du, Y., Chen, X., Guo, Y., Zhang, X., Zhang, H., Li, F. et al. (2021) *Phytophthora infestans* RXLR effector PITG20303 targets a potato MKK1 protein to suppress plant immunity. *New Phytologist*, 229, 501–515.

Fry, W. (2008) *Phytophthora infestans*: the plant (and R gene) destroyer. *Molecular Plant Pathology*, 9, 385–402.

Gao, X. & Shan, L. (2013) Functional genomic analysis of cotton genes with agrobacterium-mediated virus-induced gene silencing. *Methods in Molecular Biology*, 975, 157–165.

Gao, Z., Chen, Y.F., Randlett, M.D., Zhao, X.C., Findell, J.L., Kieber, J.J. et al. (2003) Localization of the Raf-like kinase CTR1 to the endoplasmic reticulum of *Arabidopsis* through participation in ethylene receptor signaling complexes. *Journal of Biological Chemistry*, 278, 34725–34732.

Gao, X., Wheeler, T., Li, Z., Kenerley, C.M., He, P. & Shan, L. (2011) Silencing *GhNDR1* and *GhMKK2* compromises cotton resistance to verticillium wilt. *The Plant Journal*, 66, 293–305.

Gao, H., Jiang, L., Du, B., Ning, B., Ding, X., Zhang, C. et al. (2022) GmMKK4-activated GmMPK6 stimulates GmERF113 to trigger resistance to *Phytophthora sojae* in soybean. *The Plant Journal*, 111, 473–495.

Haas, B.J., Sophien, K., Zody, M.C., Jiang, R.H.Y., Handsaker, R.E., Cano, L.M. et al. (2009) Genome sequence and analysis of the Irish potato famine pathogen *Phytophthora infestans*. *Nature*, 461, 393–398.

Hays, D.B., Reid, D.M., Yeung, E.C. & Pharis, R.P. (2000) Role of ethylene in cotyledon development of microspore-derived embryos of *Brassica napus*. *Journal of Experimental Botany*, 51, 1851–1859.

He, X., Wang, C., Wang, H., Li, L. & Wang, C. (2020) The function of MAPK cascades in response to various stresses in horticultural plants. *Frontiers in Plant Science*, 11, 952.

Helderman, T.A., Deurhof, L., Bertran, A., Richard, M.M.S., Kormelink, R., Prins, M. et al. (2022) Members of the ribosomal protein S6 (RPS6) family act as pro-viral factor for tomato spotted wilt orthotospovirus infectivity in *Nicotiana benthamiana*. *Molecular Plant Pathology*, 23, 431–446.

Hoser, R., Żurczak, M., Lichocka, M., Zuzga, S., Dadlez, M., Samuel, M.A. et al. (2013) Nucleocytoplasmic partitioning of tobacco N receptor is modulated by SGT1. *New Phytologist*, 200, 158–171.

Ivanov, A.A., Ukladov, E.O. & Golubeva, T.S. (2021) *Phytophthora infestans*: an overview of methods and attempts to combat late blight. *Journal of Fungi*, 7, 1071.

Jones, J.D. & Dangl, J.L. (2006) The plant immune system. *Nature*, 444, 323–329.

Katou, S., Yamamoto, A., Yoshioka, H., Kawakita, K. & Doke, N. (2003) Functional analysis of potato mitogen-activated protein kinase kinase, StMEK1. *Journal of General Plant Pathology*, 69, 161–168.

Komis, G., Šamajová, O., Ovečka, M. & Šamaj, J. (2018) Cell and developmental biology of plant mitogen-activated protein kinases. *Annual Review of Plant Biology*, 69, 237–265.

Li, G., Meng, X., Wang, R., Mao, G., Han, L., Liu, Y. et al. (2012) Dual-level regulation of ACC synthase activity by MPK3/MPK6 cascade and its downstream WRKY transcription factor during ethylene induction in *Arabidopsis*. *PLoS Genetics*, 8, e1002767.

Li, L., Li, M., Yu, L., Zhou, Z., Liang, X., Liu, Z. et al. (2014) The FLS2-associated kinase BIK1 directly phosphorylates the NADPH oxidase RbohD to control plant immunity. *Cell Host and Microbe*, 15, 329–338.

Li, N., Han, X., Feng, D., Yuan, D. & Huang, L.J. (2019) Signaling crosstalk between salicylic acid and ethylene/jasmonate in plant defense: do we understand what they are whispering? *International Journal of Molecular Sciences*, 20, 671.

Li, T., Wang, Q., Feng, R., Li, L., Ding, L., Fan, G. et al. (2019) Negative regulators of plant immunity derived from cinnamyl alcohol dehydrogenases are targeted by multiple *Phytophthora* Avr3a-like effectors. *New Phytologist*. Available from: https://doi.org/10.1111/nph.16139

Li, T., Zhang, H., Xu, L., Chen, X., Feng, J., Wu, W. et al. (2022) StMPK7 phosphorylates and stabilizes a potato RNA-binding protein StUBA2a/b to enhance plant defence responses. *Horticulture Research*, 9, uhac177.

Li, X., Zhang, Y., Huang, L., Ouyang, Z., Hong, Y., Zhang, H. et al. (2014) Tomato SlMKK2 and SlMKK4 contribute to disease resistance against *Botrytis cinerea*. *BMC Plant Biology*, 14, 166.

Liebrand, T.W.H., van den Berg, G.C.M., Zhang, Z., Smit, P., Cordewener, J.H.G., America, A.H.P. et al. (2013) Receptor-like kinase SOBIR1/EVR interacts with receptor-like proteins in plant immunity against fungal infection. *Proceedings of the National Academy of Sciences of the United States of America*, 110, 10010–10015.

Liu, Y. & Zhang, S. (2004) Phosphorylation of 1-aminocyclopropane-1-carboxylic acid synthase by MPK6, a stress-responsive mitogen-activated protein kinase, induces ethylene biosynthesis in Arabidopsis. *The Plant Cell*, 16, 3386–3399.

Liu, Z.Q., Liu, Y.Y., Shi, L.P., Yang, S., Shen, L., Yu, H.X. et al. (2016) SGT1 is required in PcINF1/SRC2-1 induced pepper defense response by interacting with SRC2-1. *Scientific Reports*, 22, 21651.

Ma, L. & Borhan, M.H. (2015) The receptor-like kinase SOBIR1 interacts with *Brassica napus* LepR3 and is required for *Leptosphaeria maculans* AvrLm1-triggered immunity. *Frontiers in Plant Science*, 6, 933.

Mase, K., Mizuno, T., Ishihama, N., Fujii, T., Mori, H., Kodama, M. et al. (2012) Ethylene signaling pathway and MAPK cascades are required for AAL toxin-induced programmed cell death. *Molecular Plant-Microbe Interactions*, 25, 1015–1025.

Matsukawa, M., Shibata, Y., Ohtsu, M., Mizutani, A., Mori, H., Wang, P. et al. (2013) *Nicotiana benthamiana calreticulin* 3a is required for the ethylene-mediated production of phytoalexins and disease resistance against oomycete pathogen *Phytophthora infestans*. *Molecular Plant-Microbe Interactions*, 26, 880–892.

Meng, X. & Zhang, S. (2013) MAPK cascades in plant disease resistance signaling. *Annual Review of Phytopathology*, 51, 245–266.

Ouyang, Z., Li, X., Huang, L., Hong, Y., Zhang, Y., Zhang, H. et al. (2015) Oligandrins induce resistance in tomato. *Molecular Plant Pathology*, 16, 238–250.

Pitzschke, A., Schikora, A. & Hirt, H. (2009) MAPK cascade signalling networks in plant defence. *Current Opinion in Plant Biology*, 12, 421–426.

Popescu, S.C., Popescu, G.V., Bachan, S., Zhang, Z., Gerstein, M., Snyder, M. et al. (2009) MAPK target networks in *Arabidopsis thaliana* revealed using functional protein microarrays. *Genes & Development*, 23, 80–92.

Postma, J., Liebrand, T.W.H., Bi, G., Evrard, A., Bye, R.R., Mbengue, M. et al. (2016) Avr4 promotes Cf-4 receptor-like protein association with the BAK1/SERK3 receptor-like kinase to initiate receptor endocytosis and plant immunity. *New Phytologist*, 210, 627–642.

Shibata, Y., Ojika, M., Sugiyama, A., Yazaki, K., Jones, D.A., Kawakita, K. et al. (2016) The full-size ABCG transporters Nb-ABCG1 and Nb-ABCG2 function in pre- and postinvasion defense against *Phytophthora infestans* in *Nicotiana benthamiana*. *The Plant Cell*, 28, 1163–1181.

Smekalova, V., Luptovciak, I., Komis, G., Samajova, O., Ovecka, M., Doskocilova, A. et al. (2014) Involvement of YODA and mitogen activated protein kinase 6 in *Arabidopsis* post-embryogenic root development through auxin up-regulation and cell division plane orientation. *New Phytologist*, 203, 1175–1193.

Van der Does, D., Leon-Reyes, A., Koornneef, A., Van Verk, M.C., Rodenburg, N., Pauwels, L. et al. (2013) Salicylic acid suppresses jasmonic acid signaling downstream of SCFCOI1-JAZ by targeting GCC promoter motifs via transcription factor ORA59. *The Plant Cell*, 25, 744–761.

Wang, K., Uppalapati, S.R., Zhu, X., Dinesh-Kumar, S.P. & Mysore, K.S. (2010) SGT1 positively regulates the process of plant cell death during both compatible and incompatible plant–pathogen interactions. *Molecular Plant Pathology*, 11, 597–611.

Wang, H., Chen, Y., Wu, X., Long, Z., Sun, C., Wang, H. et al. (2018) A potato STRUBBELIG-RECEPTOR FAMILY member, StLRPK1, associates with StSERK3A/BAK1 and activates immunity. *Journal of Experimental Botany*, 69, 5573–5586.

Xu, J., Li, Y., Wang, Y., Liu, H., Lei, L., Yang, H. et al. (2008) Activation of MAPK kinase 9 induces ethylene and camalexin biosynthesis and enhances sensitivity to salt stress in *Arabidopsis*. *Journal of Biological Chemistry*, 283, 26996–27006.

Yang, X., Chen, L., Yang, Y., Guo, X., Chen, G., Xiong, X. et al. (2020) Transcriptome analysis reveals that exogenous ethylene activates immune and defense responses in a high late blight resistant potato genotype. *Scientific Reports*, 10, 21294.

Zhang, S. & Liu, Y. (2001) Activation of salicylic acid-induced protein kinase, a mitogen-activated protein kinase, induces multiple defense responses in tobacco. *The Plant Cell*, 13, 1877–1889.

Zhang, M. & Zhang, S. (2022) Mitogen-activated protein kinase cascades in plant signaling. *Journal of Integrative Plant Biology*, 64, 301–341.
Zhang, M., Su, J., Zhang, Y., Xu, J. & Zhang, S. (2018) Conveying endogenous and exogenous signals: MAPK cascades in plant growth and defense. *Current Opinion in Plant Biology*, 45, 1–10.
Zhang, H., Li, F., Li, Z., Cheng, J., Chen, X., Wang, Q. et al. (2021) Potato StMPK7 is a downstream component of StMKK1 and promotes resistance to the oomycete pathogen *Phytophthora infestans*. *Molecular Plant Pathology*, 22, 644–657.

SUPPORTING INFORMATION

Additional supporting information can be found online in the Supporting Information section at the end of this article.

How to cite this article: Yang, H., Chen, X., Yang, R., Cheng, J., Chen, Y., Joosten, M.H.A.J. et al. (2023) The potato StMKK5-StSIPK module enhances resistance to *Phytophthora* pathogens through activating the salicylic acid and ethylene signalling pathways. *Molecular Plant Pathology*, 24, 399–412. Available from: https://doi.org/10.1111/mpp.13306